

U.S. DEPARTMENT OF THE INTERIOR  
U.S. GEOLOGICAL SURVEY

The relationship between the Porco, Bolivia,  
Ag-Zn-Pb-Sn deposit and the Porco caldera

by

Charles G. Cunningham<sup>1</sup>, Hugo Aparicio N.<sup>2</sup>, Fernando Murillo S.<sup>3</sup>,  
Néstor Jiménez Ch.<sup>3</sup>, José Luis Lizeca B.<sup>3</sup>, Edwin H. McKee<sup>4</sup>,  
George E. Ericksen<sup>5</sup>, and Franz Tavera V.<sup>3</sup>

Open-File Report 94-238

This report is preliminary and has not been reviewed for conformity with U.S. Geological Survey editorial standards and stratigraphic nomenclature.

<sup>1</sup>U.S. Geological Survey, 959 National Center, Reston, Virginia 22092

<sup>2</sup>Compañía Minera del Sur S.A., Casilla 108, Potosi, Bolivia

<sup>3</sup>Servicio Geológico de Bolivia (GEOBOL), Casilla 2729, La Paz, Bolivia

<sup>4</sup>U.S. Geological Survey, 345 Middlefield Road, Menlo Park, California 94025

<sup>5</sup>U.S. Geological Survey, 954 National Center, Reston, Virginia 22092

## **Abstract**

The Porco Ag-Zn-Pb-Sn deposit, a major Ag producer in the 16th century and currently the major Zn producer in Bolivia, consists of a swarm of fissure-filling veins in the newly recognized Porco caldera. The caldera measures 5 km N-S by 3 km E-W and formed in response to the eruption of the 12 Ma crystal-rich dacitic Porco Tuff. Well-defined topographic walls of the caldera are cut in Ordovician and Cretaceous sedimentary rocks. The mineralization is associated with, and is probably genetically related to, the 8.6 Ma Huayna Porco stock (elevation 4,528 m); the deposit is part of a system of radial dikes, metal zonation, and alteration mineral patterns centered on the stock. The outflow Porco Tuff to the north underlies the 6-9 Ma ash-flow tuffs of the Los Frailes volcanic field.

The Porco deposit consists of steeply dipping irregular and curvilinear veins that cut the intracaldera Porco Tuff about 1 km east of the Huayna Porco stock. Major veins are generally less than a meter wide and as much as 2 km long. Most of the veins, especially the most productive ones, together with a small stock, dike, and breccia pipe, are aligned along the structural margin (ring fracture) of the caldera. The ore deposit is zoned around the Huayna Porco stock--cassiterite is generally close to the stock, and base metals, mostly as sphalerite and galena, are further away, along the ring fracture veins. The primary Ag minerals, chiefly pyragyrite, acanthite, and stephanite, are most abundant in the upper parts of the veins.

Fluid inclusions in sphalerite stalactites have homogenization temperatures of about 225°C and salinities of about 8 wt. percent equivalent NaCl. The stalactites, and presence of sparse vapor-rich inclusions, suggest deposition of sphalerite under boiling conditions. Modeling the depth of formation below the water table indicates that the present ground surface is close to the surface that existed at the time of mineralization.

## **Introduction**

The Porco Ag-Zn-Pb-Sn mine has had a long history of production beginning in pre-Columbian times when Indians mined it for silver. Later, during Spanish colonial times, it was a major source of silver. Early in the current century, tin and lead were the most important commodities produced, but now Compañía Minera del Sur S.A. (COMSUR) produces zinc, lead, and silver. The deposit is currently the largest producer of zinc in Bolivia. Recent field and laboratory studies on which this report is based were a cooperative effort by the Servicio Geológico de Bolivia (GEOBOL), the U.S. Geological Survey, and COMSUR, and were funded, in part, by the Inter-American Development Bank. These studies resulted in the recognition of the presence of a small caldera and the importance of its structural margin (ring fracture) to the location of the ore deposit.

The Porco deposit is in southwestern Bolivia, in the Cordillera Oriental, about 35 km southwest of Cerro Rico de Potosi, the world's largest silver deposit (Fig. 1; Cunningham et al., 1991). The Porco mine (Fig. 2) is about 5 km south of the village

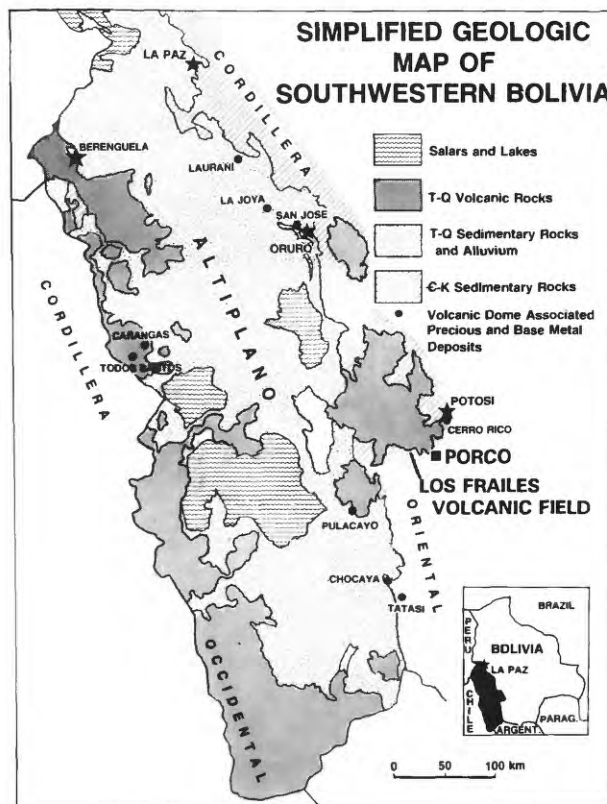


Figure 1.--Simplified geologic map of southwestern Bolivia showing the location of the Altiplano, Cordillera Oriental, Los Frailes volcanic field, Cerro Rico de Potosi deposit, and Porco deposit. T-Q, Tertiary-Quaternary; Є-K, Cambrian-Cretaceous.

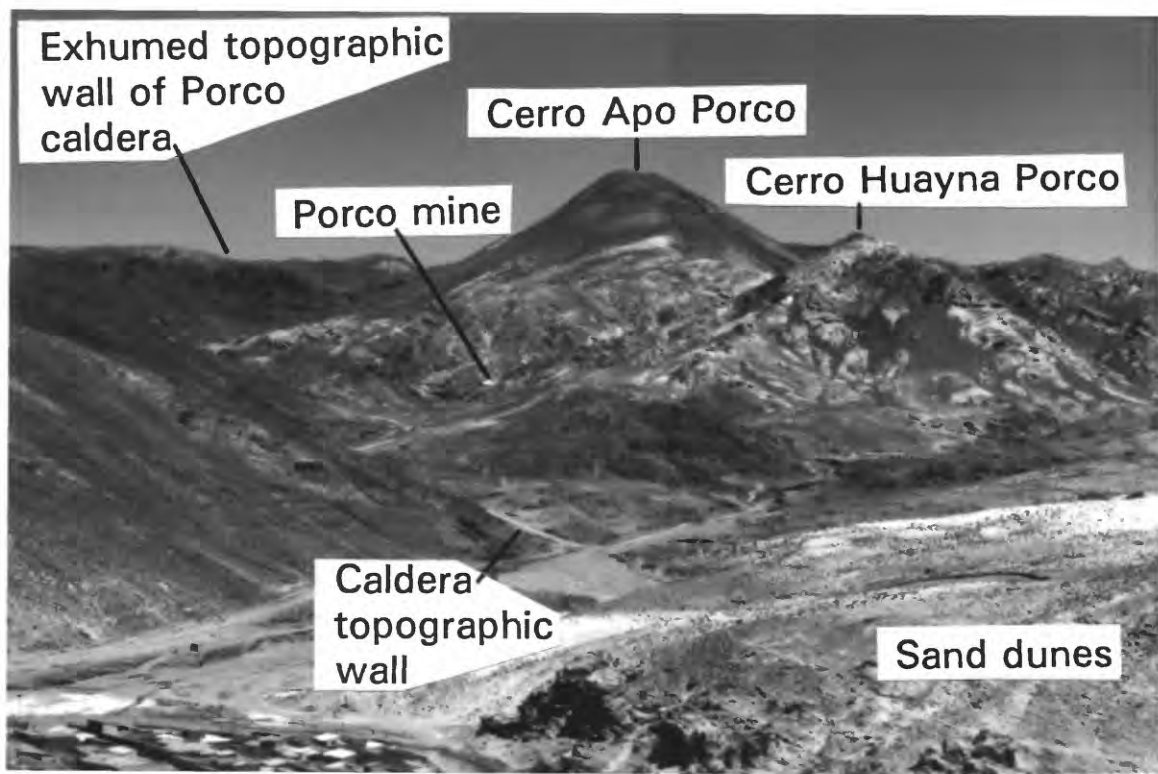


Figure 2.--Photograph looking south into the Porco caldera, taken from the village of Agua de Castilla located adjacent to the northern boundary of the geologic map (Fig. 3). It shows topographic and geologic features discussed in the text.

of Agua de Castilla, and the village of Porco is located within the caldera. The topography is dominated by two hills, Cerro Huayna Porco, elevation 4,528 m and Cerro Apo Porco, 4,886 m (Fig. 2), that are stocks within the caldera.

Published information about the Porco deposit is scanty. A 1:100,000 geologic map (Bolivia Departamento Nacional de Geología, 1964) shows the Porco volcanic rocks as part of the much larger Los Frailes volcanic field to the north. Ahlfeld and Schneider-Scherbina (1962) briefly described the Porco deposit. Jesus Rueda mapped the area in the mid-1960s and recognized that the volcanic system was independent from that of the Los Frailes volcanic field (Bolivia Departamento Nacional de Geología, 1965; Rueda, 1971). The deposit was briefly described by Sugaki and others (1983). Schneider (1985) reported on the regional geology of the Porco area and determined an age on biotite from Cerro Apo Porco as  $12.60 \pm 0.42$  Ma. Hugo Aparicio, presently the mine geologist, studied the genesis of the ore deposit for his thesis (Aparicio, 1990). The caldera and the importance of the relationship between the veins and the structural margin of a caldera were recognized during geologic mapping in November 1992 (Cunningham et al., 1993).

### **Geologic Setting**

The host rocks of the Porco caldera are Ordovician phyllites overlain by Cretaceous sandstone (Fig. 3). Black, gray, and dark-green Ordovician phyllites are widespread throughout this part of the Cordillera Oriental and have been deformed into a series of north- to northwest-trending folds cut by high-angle reverse faults (Bolivia Departamento Nacional de Geología, 1962). They are unconformably overlain by the subhorizontal lower Cretaceous Toro Toro Formation that consists of massive, strongly cross-bedded, cream to pink, medium-grained sandstone. North of the mapped area, ash-flow tuff from the Porco caldera is overlain by the 6-9 Ma rhyolitic to dacitic, predominantly peraluminous, ash-flow tuffs of the Los Frailes volcanic field. The Los Frailes tuffs were erupted from several centers and form a large ash-flow field north and west of Porco and Potosi (Fig. 1; Ericksen and others, 1990). The northwest corner of the mapped area is covered by sand dunes (Figs. 2 and 3).

### **The Porco Caldera**

The Porco caldera (Fig. 3) formed 12 Ma (Table 1) in response to the eruption of the Porco Tuff. The fresh, moderately welded tuff (Table 2) is a medium-gray, crystal-rich dacite containing abundant phenocrysts of biotite, sanidine, quartz, and plagioclase as well as prominent pumice fragments. The intracaldera tuff is virtually homogeneous and consists mostly of one ash-flow sheet; a few small, remnants of poorly welded ash-flow tuff are present high in the intracaldera fill. Within the caldera, the tuff dips generally outward from the Apo Porco and Huayna Porco stocks. Along the south and east sides, near the topographic wall of the caldera, large slump blocks of Cretaceous sandstone, called megabreccia (Lipman,



- Contact
- — — Fault, known and inferred
- ⏟ Topographic wall of the Porco caldera
- ▨ Structural margin of the Porco caldera
- Qa Quaternary alluvium, mostly sand dunes
- Ti Intrusive rocks, mostly dacitic stocks and dikes (8.6 Ma)
- Tap Apo Porco stock (12 Ma)
- Tpi Porco Tuff, intracaldera facies (12 Ma)
- Tpo Porco Tuff, outflow facies (12 Ma)
- Ks Cretaceous sandstone
- Op Ordovician phyllite

Figure 3--Continued.

Table 1.--K-Ar age determinations of rocks related to the Porco caldera.

Sample number	Mineral dated	K <sub>2</sub> O (wt. %)	<sup>40</sup> Ar* mole/g	<sup>40</sup> Ar*/ <sup>40</sup> Ar <sup>total</sup>	Age (Ma ± 2σ)
P 5	Sanidine	10.82	1.34027x10 <sup>-10</sup>	68.9	8.6 ± 0.3
P 10	Biotite	7.06	1.22957x10 <sup>-10</sup>	61.6	12.1 ± 0.4
P 15	Biotite	8.70	1.50375x10 <sup>-10</sup>	51.6	12.0 ± 0.4

P 5 = Huayna Porco stock

P10 = Apo Porco stock

P15 = Porco Tuff

Values for constants used in calculating ages:

$${}^{40}\text{K}\lambda_{\epsilon}=0.581\times 10^{-10}\text{yr}^{-1}, \lambda_{\beta}=4.962\times 10^{-10}\text{yr}^{-1}, {}^{40}\text{K}/\text{K}=1.167\times 10^{-4}$$

Table 2.--Major-oxide and selected trace-element contents of igneous rocks from the Porco caldera. (Major-oxide and S data in weight percent. Trace-element data in parts per million.)

Field No. <u>Lab No.</u>	<u>P 3</u> <u>W-257555</u>	<u>P 4</u> <u>W-257556</u>	<u>P 5</u> <u>W-257557</u>	<u>P 10</u> <u>W-257558</u>	<u>P 15</u> <u>W-257559</u>	<u>P 19</u> <u>W-257560</u>
SiO <sub>2</sub>	67.1	65.1	65.8	67.3	66.4	63.7
Al <sub>2</sub> O <sub>3</sub>	15.4	16.2	14.9	13.3	15.1	15.8
Fe <sub>2</sub> O <sub>3</sub>	0.97	1.10	0.30	6.51	1.76	1.25
FeO	1.9	5.1	2.5	0.36	1.4	2.5
MgO	0.99	1.55	0.96	0.55	1.30	1.47
CaO	2.27	0.28	2.26	0.40	2.27	2.46
Na <sub>2</sub> O	2.42	0.33	2.14	<0.15	2.93	2.28
K <sub>2</sub> O	4.54	3.66	4.82	3.39	4.66	4.82
TiO <sub>2</sub>	0.69	0.74	0.66	0.59	0.77	0.84
P <sub>2</sub> O <sub>5</sub>	0.33	0.21	0.32	0.30	0.46	0.35
MnO	0.03	0.09	0.05	0.02	0.04	0.04
H <sub>2</sub> O <sup>+</sup>	1.3	3.8	1.8	2.2	0.78	2.1
H <sub>2</sub> O <sup>-</sup>	0.36	0.05	0.34	0.29	0.82	0.51
S	<0.01	0.58	0.03	5.1	0.03	0.01
Sc	4.63	10.20	4.48	4.12	4.49	7.68
Cr	12.2	50.8	11.5	9.9	7.8	23.6
Co	4.66	13.5	5.52	3.05	5.11	8.73
Zn	63.0	4360.0	95.6	899.0	75.3	73.
As	2.45	110.0	9.6	306.0	0.96	1.06
Rb	230.	264.	304.	290.	248.	262.
Sr	522.	<90.	521.	<70.	670.	485.
Zr	158.	170.	186.	164.	225.	238.
Mo	<2.	<3.	<3.	<3.	<3.	<3.
Sb	0.185	4.76	0.511	10.8	0.15	0.39
Cs	42.0	75.9	233.	106.8	6.70	42.3
Ba	971.	542.	1046.	155.	930.	1032.
Hf	5.36	5.60	5.34	4.82	6.38	6.09
Ta	1.54	1.40	1.55	1.53	2.34	1.62
Ag	<4	<4	<4	<4	<4	<4
Be	5	4	5	4	5	3
Bi	<20	<20	<20	<20	<20	<20
Ga	25	22	24	20	26	25
Sn	<10	29	<10	32	<10	<10
Au	.002	.002	<.002	.002	<.002	<.002
Th	21.3	16.5	21.9	20.7	25.8	21.0
U	5.16	4.40	6.16	5.01	6.10	5.21

Major-element data by X-ray fluorescence, J. S. Mee and D. F. Siems, analysts. Most trace-element data by instrumental neutron activation analysis, J. Grossman, analyst; Ag, Be, Bi, Ga, and Sn by induction coupled plasma optical spectroscopy, P.H. Briggs, analyst; Au by graphite furnace atomic absorption, H. Smith, analyst. P 3 = breccia pipe; P 4 = propylitized Porco Tuff from west of Cerro San Cristobal; P 5 = Huayna Porco stock; P 10 = Apo Porco stock; P 15 = fresh Porco Tuff from near the village of Porco; and P 19 = sericitized Porco Tuff wall rock from within the mine area southeast of Cerro Huayna Porco. Locations shown on geologic map, Figure 3.

1976), are embedded in the tuff. A vertical drill hole, within the caldera, about 1 km northwest of Cerro Apo Porco, started in tuff but passed through the tuff and into the underlying phyllites at a depth that shows the southern topographic wall dips northward about 60°. The bowl-shaped topographic wall along the north side of the caldera is well exposed in cross section just east of the main road leading north from the town of Porco. The wall here is underlain by Ordovician phyllite; Porco Tuff, with a subhorizontal compaction foliation, is ponded against it. The topographic wall here dips 35° into the caldera. An excellent exposure of the caldera's topographic wall is the northwest-facing escarpment about 1 km northeast of Cerro Apo Porco (Fig. 2). The intracaldera tuff is at least 370 m thick. Three holes were drilled about 370 m deep in the vicinity of small stock about 1 km east of Cerro Huayna Porco, and each bottomed in tuff.

The Porco Tuff is variably altered within the caldera but is generally freshest in the northern part. A representative sample collected near the village of Porco (P15, Fig. 3) contains about 70 percent phenocrysts of euhedral black biotite, resorbed beta-morphology quartz, Carlsbad-twinned sanidine, and plagioclase in a matrix of ash, pumice, and lithic fragments. Fragments of the country rock are scattered throughout the tuff. An alteration halo centered on the Huayna Porco stock shows mineralogic changes in the tuff that reflect variations in the intensity of alteration. Near the stock, and especially in the vicinity of the veins, the feldspars and groundmass of the tuff contain sericite (sample P19). Outward from the Huayna Porco stock, beyond the veins, a transition zone characterized by propylitically altered rocks (Table 2, sample P4) surrounds the sericitically altered rocks and grades laterally outward into fresh rocks.

Subhorizontal outflow Porco Tuff occurs as patches west of the caldera (Fig. 3) and is present along the north edge of the mapped area, north of Río Aqua de Castilla, where it is covered by younger Los Frailes tuffs.

The intracaldera Porco Tuff is cut by the Apo Porco and Huayna Porco stocks as well as by smaller stocks and dikes (Fig. 3). The Apo Porco stock at the southern margin of the caldera (Tap, Fig. 3) is the largest and forms the highest hill in the mine area. There is no evidence of notable mineral deposits associated with the Apo Porco stock (Bolivia Departamento Nacional de Geología, 1965). The smaller Huayna Porco stock is near the center of the caldera and is surrounded by a series of radiating dikes and veins. Biotite from the Apo Porco stock has been dated at  $12.1 \pm 0.4$  Ma (Table 1) and thus is essentially the same age as the Porco Tuff. In contrast, sanidine from the Huayna Porco stock gives an age of  $8.6 \pm 0.3$  Ma. All of the intrusive rocks contain a similar mineral assemblage. The Apo Porco stock consists mostly of fresh, light gray dacite (sample P10, Table 2). It contains phenocrysts of biotite, resorbed beta-morphology quartz, plagioclase, and large (up to several centimeters) Carlsbad-twinned sanidine crystals in a fine-grained matrix of the same mineral assemblage. Mirolitic cavities are conspicuous. The Huayna Porco stock, as

well as a small stock about 1 km east of Cerro Huayna Porco, and the dikes have virtually the same mineral assemblage as the Apo Porco stock. Biotite is the dominant mafic mineral but it is locally altered to sericite and opaque minerals. A few relict hornblende crystals are present. Plagioclase is commonly sericitized, but the large sanidine phenocrysts are generally fresh.

A breccia pipe (sample P3, Table 2) crops out about 1 km west of Cerro San Cristobal; it contains fragments having the same phenocryst assemblage as the Porco Tuff, a black glass matrix, lithic fragments, large pumice fragments, and a few rounded boulders of a dacite. Chemical analyses of the Apo Porco stock (P10), Huayna Porco stock (P5), and matrix of the breccia pipe (P3) are shown in Table 2.

### **Ore Deposits**

The Porco deposit is currently (1993) producing Ag-bearing Zn-Pb ores at the rate of 1,200 metric tons per day, which yield a monthly total of 6,200 tonnes of Zn concentrate, averaging 49.5 percent Zn and 400 g/t Ag, and 290 tonnes of Pb concentrate, averaging 60 percent Pb and 3,500 g/t Ag. Present mine reserves are 2.1 million tonnes of ore averaging 15 percent Zn, 1.5 percent Pb, and 175 g/t Ag (COMSUR, written communication, February 1993). Ore grades and concentrations of selected trace elements are given in Table 3.

Ore is principally present in well-defined, steeply dipping veins that cut the intracaldera Porco Tuff. Most of the major veins (Fig. 3) crop out at the surface. The veins tend to be curvilinear and have sharp contacts with the wall rocks; major veins are generally less than a meter wide, but locally are up to 3 meters wide, and extend up to 2 km in length. The ores range from massive monomineralic to multimineralic, banded, and locally crustiform and vuggy. The San Antonio vein, one of the principal producing veins in the mine, dips  $\sim 70^\circ$  E and has been mined vertically for over 400 m. The nearby Larga vein is mostly vertical. The vein structures continue below the depth of mining, which presently is at the 3,980 level on the San Antonio vein. It has long been known that many of the veins were curved, especially some of the highly productive ones such as the San Antonio vein. The vein systems near Cerro Milagro, near the southwest margin, trend northwest, whereas the Panfilo vein, just to the east, is arcuate and trends east-west (Fig. 3).

Metal zoning is well defined. Sn, principally as cassiterite, is most abundant near the Huayna Porco stock. Pb and Zn are most abundant in the veins about 1 km east of Huayna Porco, and trace elements such as Li are most abundant farthest from the Huayna Porco stock (P16, Table 3). The change from a sericitic to a propylitic mineral assemblage in the tuff around the Huayna Porco stock coincides approximately with the outer extent of the known occurrences of the base-metal veins. Within the veins, Zn tends to be most abundant at the deeper levels and the amount of Pb and Ag increases toward the surface. Zn is present chiefly as sphalerite, which is more marmatitic with depth, and Pb is present mostly in galena. Minor quartz and pyrite

Table 3.--Ore grades and trace-element contents of samples of ore from the Porco deposit. Data in parts per million.

Field No. Lab No.	P 16 W-257561	P 18A W-257562	P 19A W-257564	P 19B W-257565	P 20A W-257567	P 20B W-257568
Mn	9700	120	210	190	220	130
Ag	<8	480	110	110	1300	3100
As	380	3800	49000	380	390	<40
Au	<.002	.011	.28	.010	.17	<.002
Be	1.5	1	<1	<1	<1	<1
Bi	<40	<40	140	<40	<40	<40
Cd	<8	1400	600	1600	640	610
Ce	56	<20	20	<20	<20	<20
Cu	20	2300	560	3300	240	190
Ga	20	15	50	7	30	<5
Li	170	20	20	<8	<8	<8
Mo	<8	<8	<8	<8	<8	<8
Pb	390	76000	3700	4600	210000	623000
Sn	<20	1400	540	190	350	530
Sr	130	430	<8	<8	30	20
Zn	1300	504000	201000	536000	196000	184000

Most trace-element data by induction coupled plasma-atomic emission spectroscopy, P. H. Briggs, analyst; Be and Ga by DC arc atomic emission spectroscopy, R.T. Hopkins, analyst; Au by graphite furnace atomic absorption, D. M. Hopkins, analyst. P 16 = peripheral vein. P 18 = San Antonio vein, deepest level of mine, 195 level, 3,980 m elevation, mine coordinates 10,950N, 12,000E, 18A = sphalerite and galena. P 19 = Claudia vein, Juan Carlos level, 4,219 m elevation, mine coordinates 10,530N, 12,100E, P 19A = pyrite breccia, P 19B = massive sphalerite. P 20 = San Antonio vein, Santa Cruz level, 4,410 m elevation, mine coordinates, 10,530N, 11,457E, P 20A = galena and pyrite, P 20B = galena. Sample locations and projected locations from underground workings are shown on geologic map, Figure 3.

are generally ubiquitous. Primary Ag minerals, principally pyragyrite, acanthite, and stephanite, increase upward in the veins. The near-surface oxide ores contain limonite and cerussite; Ag-rich oxide ores, now mined out, were the sources of large amounts of Ag in the 16th century. In the paragenetic sequence, cassiterite is early and present as equant crystals and as acicular aggregates (needle tin) with sphalerite.

Arsenopyrite, followed by chalcopyrite, stannite, sphalerite, and galena (with variable amounts of Ag), was deposited after the cassiterite. Ag and Pb sulfosalts, including stephanite and semseyite, are the youngest of the primary minerals. Gold has not been discovered in economic quantities in the deposit; however, vein samples (Table 3) contain up to 0.28 ppm Au.

Sphalerite stalactites have been found at one locality in the Porco mine. Two samples were collected from a cavity in the Santa Ana vein on the San Cayentano level (4,184 m). The larger stalactite (Fig. 4) has an axial tube about 1.3 cm in diameter, which is lined with a 1-mm layer of granular sphalerite, quartz, and chalcopyrite. This layer is surrounded by a zone of dark-brown sphalerite about 0.5 cm thick and then by an outer zone of honey-brown sphalerite, also about 0.5 cm thick. The sphalerite zones consist of successive layers that show oscillatory color banding. The sphalerite crystals have well-developed crystal faces that point radially outward from the axial tube. The second, a smaller specimen, about 1 cm by 2 cm, consists of three stalactites grown together (Fig. 5). The color zonation of the smaller specimen is the opposite of the large one. Liquid-rich fluid inclusions in the large stalactite have homogenization temperatures of 221-235°C and salinities of ~10 wt. percent equivalent NaCl. Fluid inclusions in the small stalactites are similar to those in the large stalactite and have homogenization temperatures of 219-228°C and salinities of 7-8 wt. percent equivalent NaCl; the averages are ~225°C and 8 wt. percent equivalent NaCl. Vapor-rich inclusions appear to be locally present, but their strong internal reflectance makes them difficult to document.

### Discussion

The Porco caldera formed 12.0 Ma as a result of collapse of the magma chamber when the Porco Tuff was erupted. The collapse occurred along a structural margin, or ring fracture zone, during eruption. The ring fracture, at least on the eastern side of the caldera, dipped vertically to ~70° outward with depth. As the eruption progressed, large blocks broke away from the upper part of the oversteepened margin to form megabreccia blocks within the tuff. The resulting landslide scars now form the bowl-shaped topographic walls of the caldera. Continued eruptions filled the caldera with tuff. The caldera has not been extensively modified by erosion since it was formed. Evidence for this includes the presence of outflow Porco Tuff, the bottom contact of which defines the topographic surface at the time of the eruption. Additional field evidence comes from the presence of miarolitic cavities in the Apo Porco stock, which intruded and domed the intercaldera tuff



Figure 4.--Photograph of sphalerite stalactite from the Porco mine. The stalactite is about 4 cm in diameter.

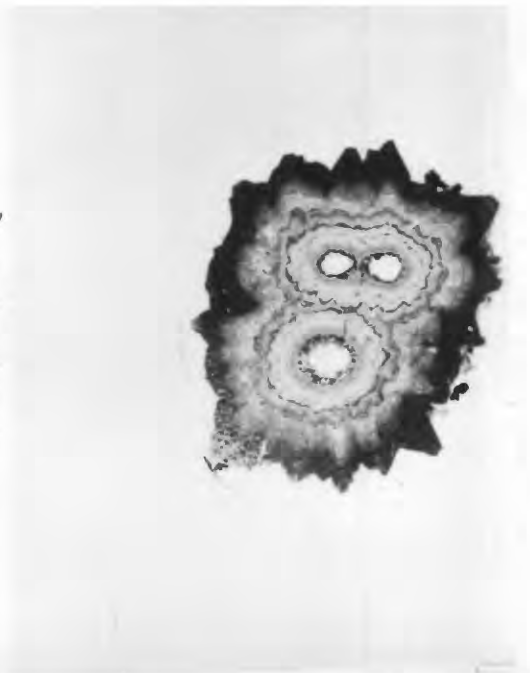
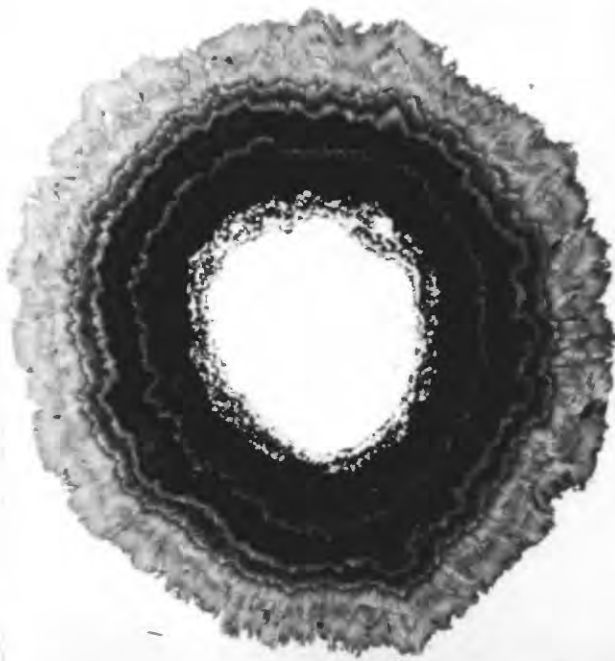


Figure 5.--Doubly polished plates showing cross sections of sphaerite stalactites from the Porco mine. The large stalactite on the left is the same as that shown in Figure 4.

shortly after eruption.

Hydrothermal alteration and mineralization were closely associated with the Huayna Porco stock. This stock, which also caused doming of the Porco Tuff, is surrounded by a system of radial dikes and a zoned alteration mineral assemblage that is coincident with a zoned metal assemblage in the tuff; all of these closely related processes took place at essentially the same time, about 8.6 Ma. The chemistry and mineralogy of the Huayna Porco stock are similar to those of the older Porco Tuff and Apo Porco stock (Table 2), and all of the Porco rocks and Los Frailes tuffs are peraluminous. The position of the Huayna Porco stock, in the center of the caldera, and the similarities of chemistry and mineralogy would suggest that the Porco rocks are all part of the same magmatic system and that the Huayna Porco stock was a resurgent stock emplaced near the end stages of the caldera cycle (Smith and Bailey, 1968). However, the 3.4 Ma age difference between the stock and the tuff is too long to keep a magmatic system active and indicates that a new, Los Frailes age, magmatic-hydrothermal system formed and was superimposed on the earlier caldera system.

The position of the buried structural margin of the caldera is interpreted to consist of two nested, annular, ring-fracture zones, as indicated on Figure 3. The surface expression of the buried structural margin is a composite of several features, including curved veins, a small stock, an arcuate dike, a breccia pipe, and altered and mineralized tuff as shown on Figure 3. The small dacitic stock located 1 km east of Cerro Huayno Porco is interpreted to be the feeder for an eroded ring dome along the structural margin. The structural margin along the northeast side of the caldera is marked by the presence of a dike that is perpendicular to the nearby radial dikes that partly surround the Huayna Porco stock, and by a breccia pipe (sample P 3, Table 2). The northern structural margin is not as well delineated. The western side of the structural margin is interpreted to be in the arcuate valley that trends north from Cerro Milagro. That interpretation is based on several parameters: (1) the geometry of structural margins as compared to those mapped in other calderas, (2) the projection of the structural margin from where its presence is better defined, (3) the alignment of areas of altered rock and associated small mineral deposits along this valley that reflect leakage of the hydrothermal fluids along a structural control, and (4) the arcuate form of the valley that probably reflects the local erosion of the more altered rocks. This projection of the structural margin along the west side of the Huayna Porco stock is important because if the fracture system in the tuff above the structural margin was significantly open to hydrothermal fluids at the time of mineralization, this area may be an important exploration target.

Both regional and local structures have had an important role in both the caldera development and mineralization. Two northwest-trending, prevolcanic, major anticlines, with a faulted syncline between them, are present in the Ordovician phyllites just south of the caldera (Bolivia Departamento Nacional de Geología, 1965).

Prominent northeasterly trending vein systems within the caldera may reflect activity that initiated the magmatic/hydrothermal activity at 8.6 Ma. An example of this structural trend may be the Larga vein, whose barren northeast extension may reflect continued reactivation after 8.6 Ma. The northeast-trending fractures may also be part of a caldera apical graben similar to the one that hosts ore at the Creede, Colorado deposit (Steven and Eaton, 1975).

Regional faulting continued after volcanism. A large fault trending N. 70°W. cuts the 6-9 Ma Los Frailes volcanic field just north of the mapped area. The Porco caldera is on the downdropped side of this fault so that the Porco caldera is now at approximately the same elevation as the younger Los Frailes tuffs to the north. Reconstruction of the pre-faulting topography indicates that the Los Frailes tuffs did not extend over the Porco area because the caldera and its associated stocks were topographic highs at the time of the Los Frailes eruptions.

The few stalactites that have been found apparently formed in a gas or vapor cavity during mineralization, indicating that the hydrothermal system was boiling. The boiling could have been brief, and much of the present mass of the stalactites could have been deposited from hydrothermal solutions that subsequently flooded the cavity; in fact, the large stalactite (Fig. 4) could be mostly overgrowth sphalerite over an earlier stalactite. Sparse vapor-rich inclusions also suggest that the system was at, or close to, boiling. The average homogenization temperature of primary fluid inclusions at 225°C and their average salinity of ~8 wt. percent equivalent NaCl are consistent with the abundance of base metals in the deposit because the base metals could have been transported as chloride complexes. A boiling 225°C, 8 wt. percent equivalent NaCl fluid, trapped under hydrostatic conditions, is consistent with a depth of ~260 meters below the water table (Haas, 1971). When this distance is added to the elevation at which they were found, it indicates that the water table at the time of mineralization was near the present ground surface and agrees with the geological interpretation that very little has been eroded from the caldera from the time of mineralization until today. Enough would have been eroded to remove any sinters, or related near-surface oxidation minerals, and to provide a source for any secondary silver minerals at the present ground surface. The only other fluid-inclusion data reported are homogenization temperatures in cassiterite of >311°C (primary) and 443-461°C (pseudo secondary) from Kelly and Turneure (1970). These samples were probably collected closer to the central Huyano Porco stock than the sphalerite samples, as is consistent with the metal zoning, and thus were covered by a higher volcanic edifice.

Other mineral deposits are known in the vicinity of Porco. Small tin placers are present in the nearby Rio Jalantaña. Unpublished Thematic Mapper images show many areas of hydrothermally altered Ordovician phyllite, mostly south of the mapped area, which may be the sites of mineral deposits. The metallogenic map of southwestern Bolivia (Claure and Minaya, 1979) indicates the presence of many Sb deposits in this area. The area is worthy of further exploration for disseminated gold,

because gold is present in the Porco ore system, gold is being mined from rocks of similar age and composition further north in the Bolivian Altiplano (Columba and Cunningham, 1993), the Ordovician phyllites in this part of Bolivia are similar to the host rocks of some Carlin-type gold deposits in Nevada, Sb is common in the uppermost parts of the Porco ore-forming system as Ag-Sb sulfosalts, and the presence of antimony deposits (Hawkins, 1982) was a significant factor in recognition and discovery of the Jerritt Canyon deposit, a major Carlin-type disseminated-Au deposit in Nevada.

### **Acknowledgments**

Many people helped to make this study possible. We especially appreciate the assistance of Carlos Birbuet for providing access to the Porco mine and sharing COMSUR mine production and reserve data, Fernando Urquidi for helping to organize the project, Edgar Velasquez for assistance in the field, Néstor Molina for providing the large sphalerite stalactite, Albrecht Schneider for sharing the results of his doctoral dissertation, Orlando Sanjinés V. for providing the small sphalerite stalactite and reference material, Timothy L. Muzik for preparing fluid-inclusion polished plates, Dorothy J. Manley for assistance with manuscript preparation, and James R. Estabrook for assistance with the graphics. Thoughtful reviews of the manuscript were kindly provided by Thomas A. Steven and Paul B. Barton, Jr. This is a contribution to IGCP Project 342 "Age and Isotopes of South American Ores."

### **References**

- Ahlfeld, Federico, and Schneider-Scherbina, Alejandro, 1964, Los yacimientos minerales y de hidrocarburos de Bolivia: Boletín No. 5 (Especial), Departamento Nacional de Geología, Ministerio de Minas y Petróleo, La Paz, Bolivia, 388 p.
- Aparicio N., Mario Hugo, 1990, Génesis del Yacimiento Minero de Porco: unpublished thesis, Departamento Geológico, Universidad Autónoma "Tomas Frias", 129 p.
- Bolivia Departamento Nacional de Geología, 1962, Cucho-Ingenio mapa Hoja No. 6434: Ministerio de Minas y Petróleo, República de Bolivia, escala 1:100,000.
- Bolivia Departamento Nacional de Geología, 1965, Porco; Levantamiento mineralógico piloto de la Cordillera y Altiplano 1962-1965, No. 16: Naciones Unidas Fondo Especial, La Paz, Bolivia, 63 p.
- Claire, H. V., and Minaya, E. R., 1979, Mineralización de los Andes Bolivianos con relación la Placa de Nazca: Memoria Explicativa, programa ERTS-Bolivia, Serie Sensoras Remotos 4, 50 p.
- Columba C., M., and Cunningham, C. G., 1993, Geologic model for the mineral deposits of the La Joya district, Oruro, Bolivia: *Economic Geology*, v. 88, p. 701-708.

- Cunningham, C. G., McNamee, J., Pinto-Vásquez, J., and Ericksen, G. E., 1991, A model of volcanic dome-hosted precious-metal deposits in Bolivia: *Economic Geology*, v. 86, p. 415-421.
- Cunningham, C. G., Aparicio N. H., Murillo S., F., Jiménez Ch., N., Lizeca B., J. L., Ericksen, G. E., and Tavera V., F., 1993, The Porco, Bolivia, Ag-Zn-Pb-Sn deposit is along the ring fracture of the newly recognized Porco caldera {abs.}: *Geological Society of America Abstracts with Program*, v. 25, no. 6, p. A-275.
- Ericksen, G. E., Luedke, R. G., Smith, R. L., Koeppen, R. P., and Urquidi B., F., 1990, Peraluminous igneous rocks in the Bolivian tin belt: *Episodes*, v. 13, p. 3-8.
- Haas, J. L., Jr., 1971, The effect of salinity on the maximum thermal gradient of a hydrothermal system at hydrostatic pressure: *Economic Geology*, v. 66, p. 940-946.
- Hawkins, R. B., 1982, Discovery of the Bell Gold mine, Jerritt Canyon District, Elko County, Nevada: *Society of Mining, Engineers of AIME*, Preprint no. 82-86, 7 p.
- Kelly, W. C., and Turneure, F. S., 1970, Mineralogy, paragenesis and geothermometry of the tin and tungsten deposits of the eastern Andes, Bolivia: *Economic Geology*, v. 65, p. 609-680.
- Lipman, P. W., 1976, Caldera-collapse breccias in the western San Juan mountains, Colorado: *Geological Society of America Bulletin*, v. 87, p. 1397-1410.
- Rueda A., Jesus, 1971, *Geología del yacimiento de Porco y sus alrededores*, Provincia Quijarro, Departamento de Potosí: Unpublished thesis, University of San Andreas, La Paz, Bolivia.
- Schneider, Albrecht, 1985, Eruptive processes, mineralization and isotopic evolution of the Las Frailes Kari Kari region/Bolivia: Unpublished Ph.D thesis, Royal School of Mines, London, England.
- Smith, R. L., and Bailey, R. A., 1968, Resurgent cauldrons: *Geological Society of America Memoir* 116, p. 618-662.
- Steven, T. A., and Eaton, G. P., 1975, Environment of ore deposition in the Creede mining district, San Juan Mountains, Colorado: I. Geologic, hydrologic, and geophysical setting: *Economic Geology*, v. 70, p. 1023-1037.
- Sugaki, A., Ueno, H., Kitakaze, A., Hayashi, K., Shimada, N., Sanjines V., O., Velarde V., O.J., Sanchez, A. C., and Villena G., H., 1983, Geological and mineralogical studies on the polymetallic hydrothermal ore deposits in Andes area of Bolivia: March 1983, Sendai, Japan, 191 p.